Practical Quadrupole Theory: Quadrupole Emittance Characteristics

Randall E. Pedder
Extrel CMS L.P. ,575 Epsilon Drive, Pittsburgh, PA 15238

(Poster presented at the 51st ASMS Conference on Mass Spectrometry and Allied Topics, Montreal, Quebec, Canada, June 8 to 12, 2003)

MS/MS experiments utilizing a quadrupole coupled to a pressurized collision cell commonly use a restricted diameter aperture at the exit of a quadrupole to provide a conductance limit for the collision cell.

This presentation was created to address the following questions:

- What happens to transmission when you put a restricted aperture at the exit of a quadrupole?
- What happens to resolution when you put a restricted aperture at the exit of a quadrupole?
- What is the shape of an ion beam as it exits a quadrupole?

I. INTRODUCTION

At the previous two year's ASMS conferences, graphical introductions to quadrupole theory were presented. (1, 2) Those presentations focused on demystifying the theory associated with quadrupole operation. This presentation builds on that previous work, and is more pragmatic, seeking to explore what happens and why, when a restricted aperture is placed at the exit of a quadrupole.

Who cares? Anyone who is trying to get ions coming out of the quadrupole to go through a small aperture like the conductance limited entrance to a collision cell, that's who. So before we go any further, make a mental note of what you would guess to be the answer to the following question:

What happens to transmission if the exit aperture of a 9.5 mm quadrupole is restricted from 0.300 inches diameter to 0.050 inches, or a factor of 1/6?

If you already know the answer, then skip this presentation. If you aren't sure what should happen, you might be surprised by the experimental results.

II. THE EXPERIMENT

In a quadrupole mass spectrometer system, ions are somehow generated, focused into a quadrupole as close as possible to the centerline of the quadrupole axis, and are filtered while traveling through the quadrupole, with the resulting filtered ions traveling through an exit aperture to a detector or another analyzer. See Figure 1.

Often, an aperture is placed at the exit of a quadrupole, either to shield a detector, or to serve as a conductance limit for a collision cell. In this work, the consequences of restricting the cross section of the exit aperture were explored both theoretically through mathematical modeling, and through experimentation.

The quadrupole system with electron impact ion source used in this experiment was tuned for optimum peak shape using the standard 0.3 inch i.d. exit lens assembly for each of three separate types of experiments (faraday measurement of absolute transmission of nitrogen at m/z 28, and relative transmission curves at nitrogen m/z 28 and perfluorotributylamine at m/z 502). The same tune was used for all exit lens diameters, with slight tweaking of the exit lens only for the faraday measurements.

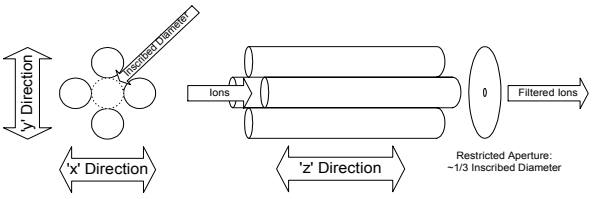


Figure 1. Schematic of quadrupole assembly identifying 'x', 'y', and 'z' directions, inscribed diameter, and ion flow.

Ion trajectories were calculated via Runge-Kutta numerical integration of the Mathieu equation using a Turbo Basic program originally developed at the University of Florida. Data were plotted using Grapher and Surfer, two plotting packages from Golden Software, Golden, Colorado.

A quadrupole constructed of 9.5 mm diameter rods with pre- and post-filters, and operated at 880 kHz was modeled and used experimentally in this work, with exit lens apertures of 0.05, 0.10, 0.15, 0.20, 0.25, and 0.3 inches (1.27, 2.54, 3.81, 5.08, 6.35, and 7.62 mm respectively).

III. PHASE SPACE ACCEPTANCE ELLIPSES

The traditional treatment of quadrupole theory starts with a derivation of the Mathieu equation from 'F=ma' all the way through to the final parameterized form, with the following parametric substitutions:

$$\frac{d^2u}{d\xi^2} + (a_u - 2q_u \cos 2\xi)u = 0 \qquad a_u = \frac{8eU}{mr_0^2\Omega^2} \qquad q_u = \frac{4eV}{mr_0^2\Omega^2}$$

The u in the above equations represents position along the coordinate axes (x or y), ξ is a parameter representing $\Omega t/2$, t is time, e is the charge on an electron, U is applied DC voltage, V is the applied zero-to-peak RF voltage, m is the mass of the ion, r is the effective radius between electrodes, and Ω is the applied RF frequency.

If one were to use numerical methods to integrate the solution to this equation, one would find some interesting correlations. It is a straightforward exercise to use Runge-Kutta numerical integration with 32 steps per RF cycle to calculate ion trajectories as well as instantaneous velocities and plot them as a function of time (See Figure 2). This figure also includes seven data points on each of the velocity and position plots, which represent points which were acquired at the exact same RF phase. 32 steps per RF cycle means every 32nd point is highlighted with a big blue dot.

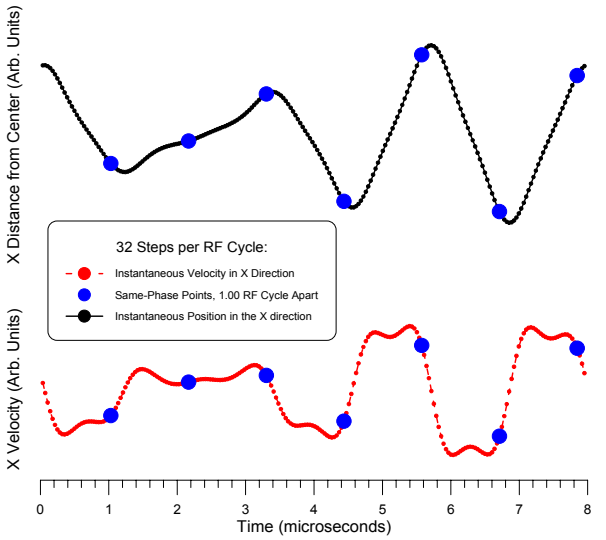


Figure 2. Calculated X direction ion trajectory and instantaneous velocity, plotted as a function of time for an ion at a= 0.271, q=0.69, (resolution=10). The seven blue dots in each plot represents a group of data points corresponding to the same RF phase.

If one plots this same data set with X position on the X axis and X velocity on the Y axis, these seven 'same-phase' data points are seen to fall onto an ellipse. (See Figure 3.)

Note that the trajectory seemingly takes a random walk around X-Xdot phase space, and just

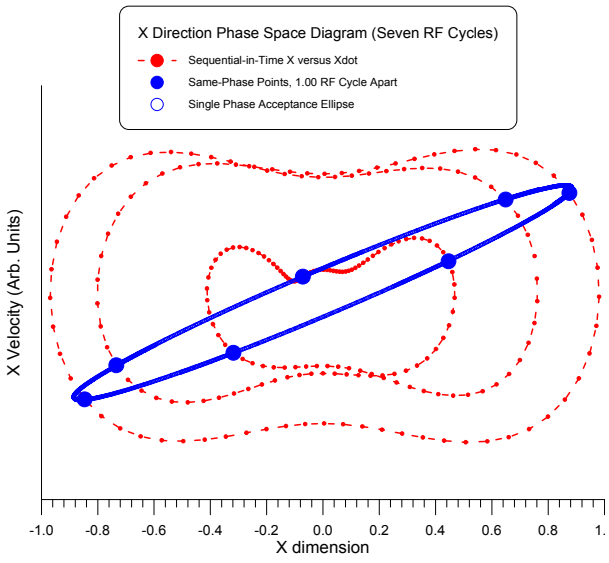


Figure 3. Calculated X direction ion trajectory and instantaneous velocity, plotted against each other for an ion at a= 0.271, q=0.69, (resolution=10). The seven blue dots in each plot represents a group of data points corresponding to the same RF phase.

'conveniently' lands on the same ellipse every 32 steps

In fact, if the trajectory is calculated with an integer number of steps per RF cycle, an integer number of ellipses will appear in phase space if the trajectories are plotted as such. (See Figure 4.)

Figures 5 and 6 were generated using 1,250 data points gathered at each of thirty two steps per RF cycle, normalized such that the furthest excursion in the positional direction exactly matches the inscribed diameter of the quadrupole.

These diagrams can be interpreted such that if an ion falls on any point of one of the ellipses at its corresponding RF phase, it will be seen to process through all of the other ellipses, given enough time.

If an ion falls within said ellipse for its instantaneous phase, then it will have a theoretically stable trajectory through the quadrupole, with a proportionally smaller set of ellipses.

What is interesting is that there is a sweet spot centered around the origin of the diagram representing the superposition of all of the phase space acceptance ellipses. An ion injected into the quadrupole with minimal angle, and close to the center will have a stable trajectory through the quadrupole, regardless of RF phase. This sweet spot is often referred to as the acceptance of the quadrupole.

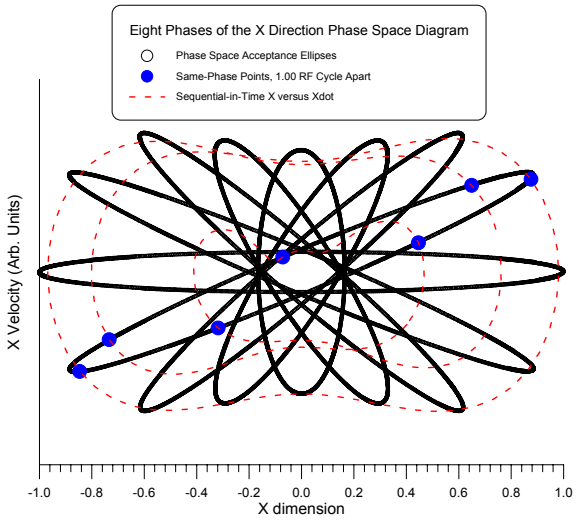


Figure 4. Calculated X direction ion trajectory and instantaneous velocity, plotted as a function of time for an ion at a= 0.271, q=0.69, (resolution=10). The seven blue dots in each plot represents a group of data points corresponding to the same RF phase.

Consider the velocity = 0 axis. If one were to segment that axis into two hundred steps, and then for each step along the velocity = 0 axis, calculate how many of 100 phase space acceptance ellipses include that step. Such a histogram would show 100% at the center, and taper off to zero at the poles. The solid lines in figures 7 and 8 illustrate this distribution.

Similarly one could correlate the maximum excursion of each of the ellipses, regardless of angular velocity, and calculate a similar set of histograms. One could speculate that these two pairs of histograms represent the range of probabilities for where ions are at any given moment in time.

One could further calculate a three-dimensional surface by scaling each of the X and Y histograms by each other to create a three-dimensional array, with the third dimension being a scaled probability of ion signal for that pair of x-y coordinates.

Figures 9 and 10 represent these three-dimensional representations for the zero-velocity crossing model and the maximum excursion model, respectively, with figures 11 and 12 representing the same data sets viualized as an image current at the exit of the quadrupole.

What is notable is that these models each suggest that the ion beam is concentrated along a plus-sign that connects opposite poles, with minimal ion signal along the asymptotes of the poles. This has been established by numerous researchers in the past, including detailed computer simulations by Joe Campana in 1980 (3), as well as experimentally measured ion burn images on a surface by Kane, Angelico and Wysocki (4). As well, numerous researchers have viewed the ion beam directly using a microchannel plate and phosphor screen (5, 6, 7).

Figure 13 is taken from Kane, Angelico and Wysocki (4), and matches nicely with the plus sign image current modeled in figures nine through twelve. This image is a photograph of a surface that was placed at the exit of a quadrupole through which ions were filtered to bombard the surface. Presumably, the quadrupole was oriented such that the asymptotes of the quadrupole were towards the corners of the photograph, and the poles were left/right/top/bottom.

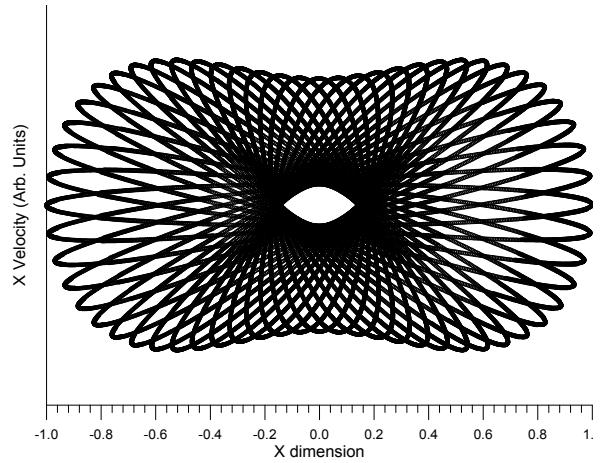


Figure 5. X-Direction phase space diagram showing thirty-two acceptance ellipses.

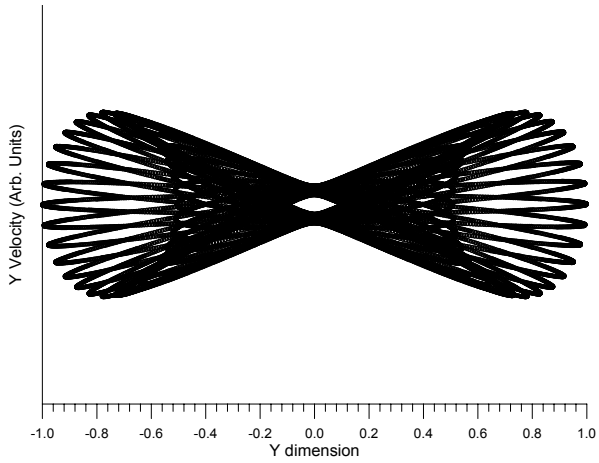


Figure 6. Y-Direction phase space diagram showing thirty-two acceptance ellipses.

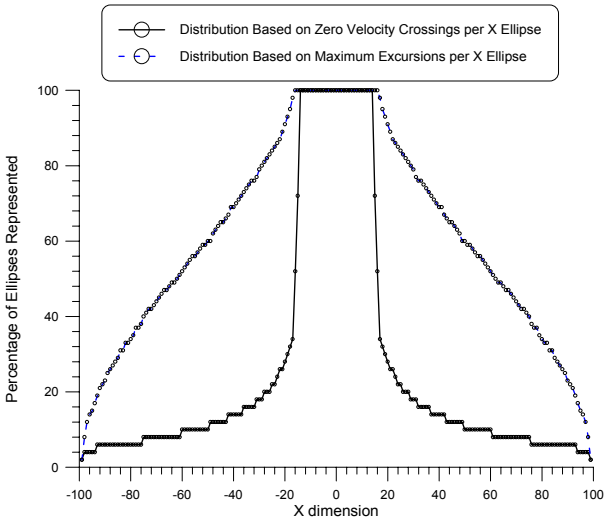


Figure 7. Calculated positional distribution in the X direction for ions that have stable trajectories that barely graze the inscribed diameter of the quadrupole, based on one hundred-phase space acceptance ellipses..

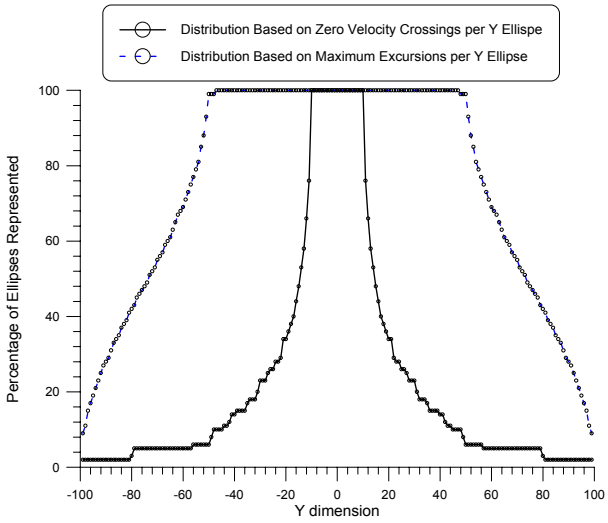


Figure 8. Calculated positional distribution in the Y direction for ions that have stable trajectories that barely graze the inscribed diameter of the quadrupole, based on one hundred-phase space acceptance ellipses..

IV. APERTURE SIZE EFFECTS ON TRANSMISSION

The absolute transmission of a quadrupole was measured using a single quadrupole with six different exit aperture sizes, ranging from 0.050 inches to the standard 0.300 inches.

So here is where we see how good your guess was…

If you guessed that transmission goes proportional with aperture diameter, then you were wrong. It is not 1/6.

If you guessed that transmission goes proportional with aperture cross-sectional area, then you are on the right track. The ratio of cross-sectional areas was a factor of 36, and the measured result was a factor of 49 reduction in transmission. (See Figure 14.)

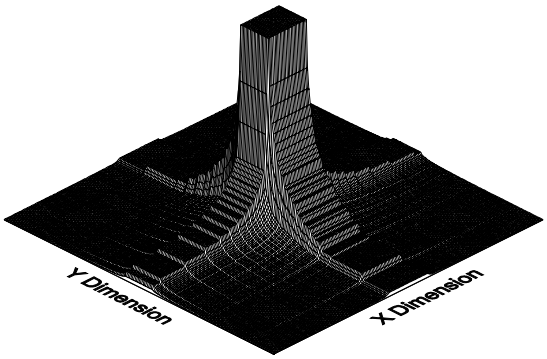


Figure 9. Three-dimensional representation of calculated image current, based on zero velocity crossings distribution model. Note the 'Classic' plus sign is evident.

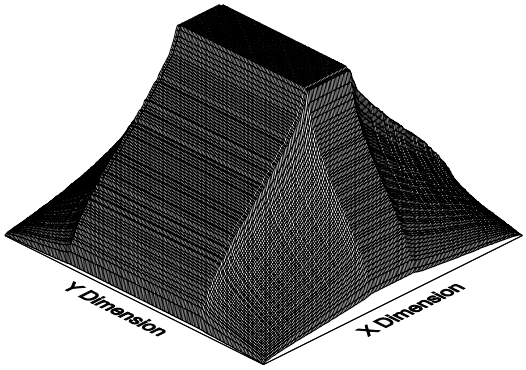


Figure 10. Three-dimensional representation of calculated image current, based on 'maximum excursion' distribution model..

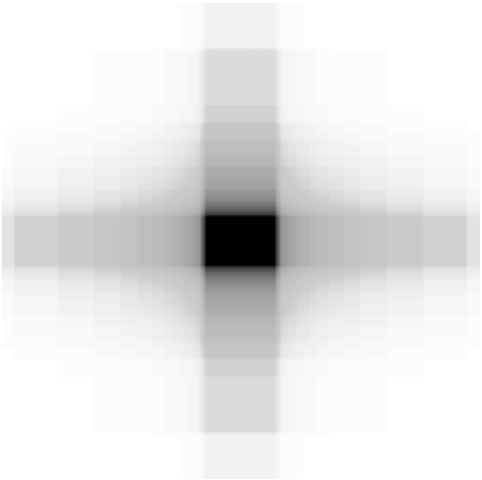


Figure 11 Calculated image current at exit of quadrupole, based on zero velocity crossings distribution model. (Same data set as figure 9) Note the 'Classic' plus sign is evident.

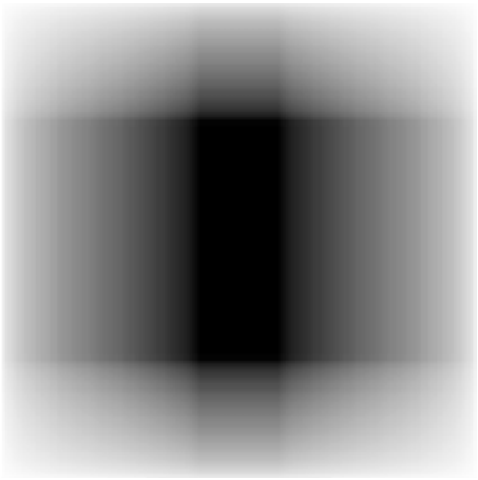


Figure 12. Calculated image current at exit of quadrupole, based on 'maximum excursion' distribution model. (Same data set as figure 10.)

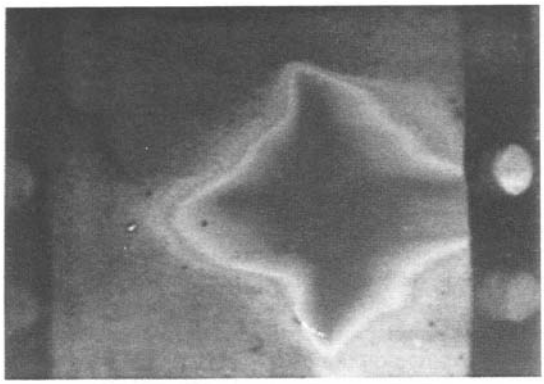


Figure 13. Condensation figure illustrating the ion beam image resulting from a four-hour bombardment of a self-assembled monolayer surface ($AuS(CH_2)_{11}OH$) with a 70 eV argon ion beam emitted from the exit of a quadrupole mass filter. (Figure taken from Figure 2a of Reference 4, by Kane, Angelico and Wysocki.)

One could theoretically estimate a relative transmission function for different apertures diameters by estimating the relative volumes cut out of the X-Y-Probability space shown in Figures 9 through 12, then calculating the relative transmission based on relative volumes.

Assuming that the 'zero-crossing' model is accurate, and calculating the relative volumes of different diameters centered around the center of the quadrupole yields the upper trace shown in figure 14 predicting mild three-fold loss in transmission with a six-fold reduction in diameter. Since that model presumes that most of the ion current is in the center, restricting the annulus would not have much impact.

Extrel CMS L.P.
575 Epsilon Drive Pittsburgh, Pennsylvania 15238-2838 USA
Tel: (412) 963-7530 FAX: (412) 963-6578 Web: www.extrel.com

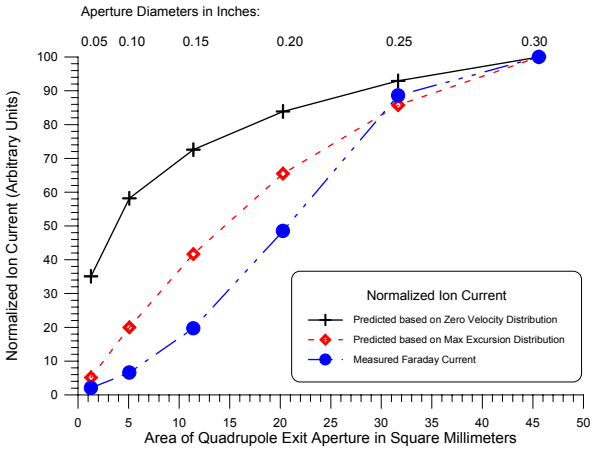


Figure 14. Theoretical and experimentally determined transmission functions as a function of exit aperture area.

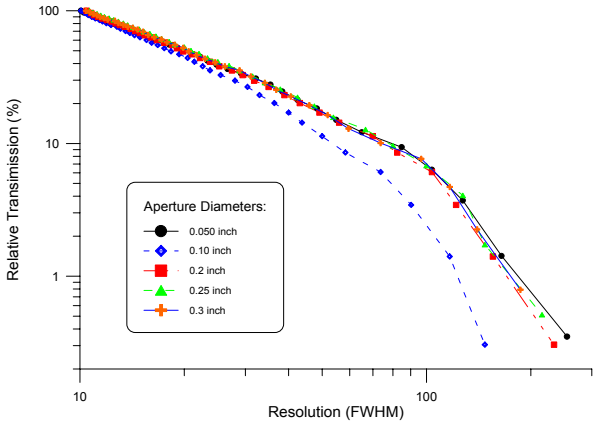


Figure 15. Resolution-transmission curves for various size apertures for m/z 28 of nitrogen. It is not clear why the -.10 inch curve doesn't match the rest, but the 0.050 diameter aperture falls in with the rest of the curves.

As I.M. Kolthoff has often been quoted, "Theory guides; experiment decides." That model does not match the experiment.

However, one could instead rationalize that most of the time the ions have non-zero velocity, and therefore they are not confined to the constricted probability plot suggested by the Zero-velocity distribution. Instead, their trajectories fall within the probability plots based on maximum excursions per each phase space ellipse, which is the opposite extreme. This model, calculated based on ratios of volumes from figures 10 and 12 for different aperture areas, yields a calculated reduction in sensitivity of around twenty-fold, compared with the experimentally determined fourty-nine-fold reduction in sensitivity.

In any case, it is clear that a modest reduction in the exit aperture diameter doesn't hurt sensitivity much. However a dramatic reduction in exit aperture size will yield a still more dramatic reduction in sensitivity.

V. APERTURE SIZE EFFECTS ON RESOLUTION

Quite surprising (at least to me), there was no profound change in observed resolution and relative transmission caused by the reduction in aperture size. However there was a noticeable reduction in signal-to-noise caused by the dramatic loss in sensitivity.

The measured resolution-transmission curves lay right on top of each other for both m/z 28 and m/z 502. (See figures 15 and 16.) This is re-assuring, since a change in relative transmission for different masses would also be an indicator of a mass discrimination effect; higher masses require higher resolution.

Since the resolution-transmission curves for different masses match so nicely, one could conclude that the sensitivity reduction associated with the reduction in aperture diameter is resolution-independent.

As an aside, it is the author's experience that

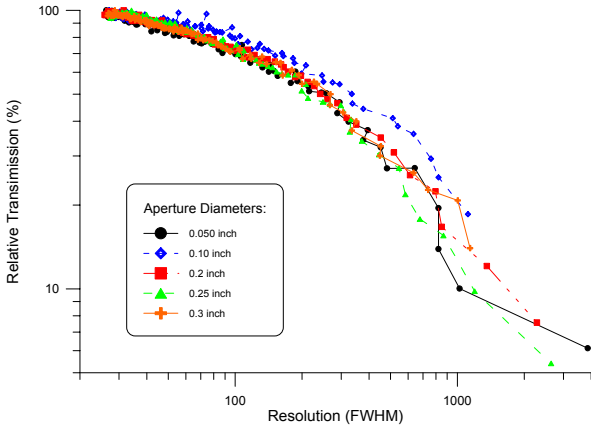


Figure 16. Resolution-transmission curves for various size apertures for m/z 502 of perfluorotributylamine. The curves overlay each other nicely, almost indistinguishable within the noise of the data.

relative transmission has been a good indicator for absolute transmission when c

different rod diameters. The caveat must be that this is true, so long as the exit aperture is approximately the same size as the inscribed diameter of the quadrupole in question, and if the emissivity of the source is much larger than the acceptance of the quadrupole.

VI. CONCLUSIONS

Restricting the quadrupole exit aperture slightly (down to 80%) from the inscribed diameter of the quadrupole causes little reduction in sensitivity, however, overall, ion transmission is approximately proportional to the area of the exit aperture.

If one requires a restricted aperture after a quadrupole, as in the case of coupling a conductance-limited collision cell to a quadrupole, then it is recommended that additional focusing lenses be used to focus the larger emissivity of the quadrupole through the limited acceptance of the aperture.

Restricting the exit aperture has only modest if not indistinguishable effects on mass resolution. This can be interpreted to mean that the reduction in transmission is independent of resolution.

Ions exiting a quadrupole have a two-dimensional cross section in the form of a plus sign which shares its asymptotes with the quadrupole, as show in theory and by experiment.

It is therefore recommended that if one is coupling two quadrupoles that they be rotationally aligned so that the quadrupoles share asymptotes as well, so that the ion beam emitted from one quadrupole will enter the second with maximum acceptance.

Measured ion currents using different aperture sizes matched the models in form, although the models under-predicted the severity of the reduction in sensitivity. However, in the modeling game, getting within a factor of two and a half isn't all that bad.

While perhaps oversimplified, a simple integration of the phase space acceptance ellipses across their velocity = 0 axis yields graphical results that correlate well with experimental evidence for emittive cross sections found in literature.

While not shown in this presentation, previous work has demonstrated that reducing the exit aperture has an additional negative side effect, in the form of noding and split peaks, especially if the ion energy is either narrowly controlled, or of high energy.(2)

VII. ADDENDUM

During the day that this poster was presented, there were some interesting discussions that warrant inclusion in this presentation.

The conclusion that restricting the exit aperture of the quadrupole will lead to dramatic losses in sensitivity holds true only for systems in which the emissivity of the ion source is much bigger than the acceptance of the quadrupole. (One of the un-written assumptions of this work.)

In contrast, there are commercial systems designs in which care has been taken to introduce ions into the very center of the quadrupole with minimal radial velocities, which have restrictive quadrupole exit apertures with no loss in sensitivity. In such a system one could conclude that the whole quadrupole isn't being used, only the center-most volume.

An additional point was made that the presented models assume that the ion beam entering the quadrupole had a uniform distribution across the inscribed diameter of the quadrupole. However in real life, the distribution of injected ions is usually much denser in the center region of the quadrupole than along its edges, which will result in ions having a higher probability of traversing the quadrupole via a smaller set of acceptance ellipses.

VIII. REFERENCES

(1) Pedder R.E. "*Practical Quadrupole Theory: Graphical Theory"*, Extrel Application Note RA_2010, Poster presented at the 49th ASMS Conference on Mass Spectrometry and Allied Topics, Chicago, IL, 2001.

(2) Pedder R.E. "*Practical Quadrupole Theory: Peak Shapes at Various Ion Energies"*, Extrel Application Note RA_2011, Poster presented at the 50th ASMS Conference on Mass Spectrometry and Allied Topics, Orlando, FL, 2001.

(3) Campana, J.E.*Int. J. Mass Spectrom. Ion Phys.* **1980***, 33,* 101.

(4) Kane, T.E., Angelico, V.J., Wysocki, V.H. "*Use of Condensation Figures to Image Low-Energy Ion Beam Damage of Monolayer Films"*, *Anal. Chem*. **1994**, *66*, 3733.

(5) Ketkar, S.N., Penn, S. Private Communication / Video Tape.

Extrel CMS L.P.
575 Epsilon Drive Pittsburgh, Pennsylvania 15238-2838 USA
Tel: (412) 963-7530 FAX: (412) 963-6578 Web: www.extrel.com

(6) Bier, M.E., Amy, J.W., Cooks, R.G., Syka, J.E.P., Ceja, P., Stafford, G. *Int. J. Mass Spectrom. Ion Processes.***1987***, 77,* 31.

(7) Short, R.T., Grimm, C.C., Todd, P.J., *J. Am. Soc. Mass Spectrom.* **1991**, *2*, 226.

Extrel CMS L.P.
575 Epsilon Drive Pittsburgh, Pennsylvania 15238-2838 USA
Tel: (412) 963-7530 FAX: (412) 963-6578 Web: www.extrel.com

Extrel
Core Mass Spectrometers